Journal of Thermal Science Vol.28, No.1 (2019) 145−157

https://doi.org/10.1007/s11630-019-1085-9 **Article ID: 1003-2169(2019)01-0145-13**

Experimental Investigation on the Effect of Mainstream Turbulence on Full Coverage Film Cooling Effectiveness for a Turbine Guide Vane

FU Zhongyi, ZHU Huiren*, CHENG Lijian, JIANG Ru

School of Power and Energy, Northwestern Polytechnical University, Xi'an 710072, China

Abstract: Experiments have been performed to investigate the effect of mainstream turbulence on the three-dimensional distribution of the full coverage film cooling effectiveness for two enlarged actual twisted vanes with cylindrical or shaped holes. The film cooling effectiveness was measured by transient liquid crystal technique at mainstream turbulence intensities of 2%, 9% and 15%. The mass flow rate ratios range from 5.5% to 12.5%. There are 3, 8 and 7 rows of film holes on the suction side, leading edge and pressure side, respectively. Results show that for the cylindrical hole vane the high mainstream turbulence intensity decreases the film cooling effectiveness in the top region and down region of pressure side in the low mass flow rate ratio of 5.5%, while the effect is opposite in the high mass flow rate ratio of 12.5%. The film cooling effectiveness in the middle region of pressure side decreases obviously with the increase of the turbulence at the low mass flow rate ratio of 5.5%, while the influence of increasing turbulence weakens gradually with the increase of mass flow rate ratio. Moreover, the high mainstream turbulence improves the film cooling effectiveness in the further downstream of the holes on suction side at the high mass flow rate ratio of 12.5%. For the shaped hole vane, the increase of mainstream turbulence decreases the film cooling effectiveness at all mass flow rate ratios. This study reveals the influence rule of the mainstream turbulence on the film cooling effectiveness in the different regions of the three-dimensional vane surface. The results would guide the designs of engineering heat transfer with application in gas turbine blade/vane cooling.

Keywords: film cooling effectiveness, turbulence intensity, mass flow rate ratio, turbine guide vane

1. Introduction

The performance of aero-engine is limited by the inlet gas temperature of the turbine components. Therefore, various cooling schemes have been used to decrease the temperature of blade and vane. Film cooling is an important technology in modern aero engines. Bunker [1] summarized the cooling technology used in turbine blade or vane. Nowadays, a better understanding of cooling technique is still required to design modern aero-engines.

In an early study of Wieghardt [2], the film cooling was used to anti icing. Then the film cooling was used on turbine engines. Goldstein [3] was the first to study the film cooling technique used in turbine blade or vane. Lots of researches have been done so far, which mainly includes two aspects: the geometric parameters of film holes and the aerodynamic parameters of mainstream and secondary flow. Andrews et al. [4] measured the heat transfer characteristics of film cooling holes with different hole pitches. Guo et al. [5] investigated the

Received: May 30, 2018 Corresponding author: ZHU Huiren E-mail: zhuhr@nwpu.edu.cn

Nomenclature

C	vane chord length/m	T_c	secondary flow temperature/K
C_p	pressure coefficient	T_g	mainstream flow temperature/K
H	vane height/m	Tu	mainstream turbulence intensity/%
MFR	mass flow rate ratio/%	T_w	wall temperature/K
P	local static pressure on vane surface/Pa	U_g	inlet flow velocity/m·s^{-1}
P_0	inlet static pressure/Pa	v'	mainstream fluctuation velocity/m·s^{-1}
P_∞^*	inlet total pressure/Pa	$\overline{v}$	mainstream average velocity/m·s^{-1}
q	surface heat flux/W·m^{-2}	**Greek symbols**	
Re	Reynolds number	λ	thermal conductivity/W·m^{-1}·K^{-1}
S	vane arc length/m	μ_g	Viscosity/kg·m^{-1}·s^{-1}
T_0	initial temperature/K	η	film cooling effectiveness
T_{aw}	adiabatic wall temperature/K	ρ_g	mainstream density/kg·m^{-3}

cooling characteristics of the fan-shaped holes on a vane. Fan-shaped holes were found to provide higher effectiveness on the suction side. However, in the far downstream of the holes on pressure side, the cylindrical holes were better. Li et al. [6] investigated the performance of dual-fanned holes. Dittmar et al. [7] compared the film cooling effectiveness of the double-row round holes with that of single-row fan-shaped holes.

The effect of aerodynamic parameters is also an important trend in film cooling studies. Thole et al. [8] studied the influence of momentum ratio on the film cooling characteristics. Nirmalan et al. [9] analyzed the influences of the mainstream turbulence intensity on film cooling performance. In the realistic condition of aero engine turbine guide vane, the mainstream inlet turbulence intensity reaches to 15%~20% [10]. Therefore, the effect of mainstream turbulence intensity becomes an important aspect in film cooling researches. The research results of Eriksen et al. [11] and Lebedev et al. [12] showed that at a relatively low momentum ratio, the high mainstream turbulence decreased film cooling effectiveness. However, the film cooling effectiveness was increased by high turbulence in high momentum ratio. Li et al. [13] investigated the influence of mainstream turbulence on the film cooling characteristics of trunk-branch hole. Schroeder et al. [14] measured the flow field and film cooling effectiveness distribution for a shaped hole on flat plate at different mainstream turbulence intensities. He found that high mainstream turbulence intensity increased the velocity undulations around the film jets and enhanced the lateral spreading.

The surface curvature has an obvious influence on the film cooling characteristics [15, 16]. Therefore, some researches were carried out on the vane or blade. Funazaki et al. [17] found that mainstream turbulence decreased the spanwise average film cooling effectiveness on the leading edge. Liu et al. [18] investigated the film cooling performance on the leading edge of a turbine guide vane.

There are multiple hole rows on real turbine vanes to achieve full coverage film cooling. Andrews [19] found that the increase of film holes improved the film cooling performance. Abdullah et al. [20] studied the thermal interaction of coolant from multiple rows of film cooling holes on flat plate at different mainstream turbulence intensities. Kingery et al. [21] studied the performance of multiple hole rows on a convex surface under different mainstream turbulences. Ames et al. [22, 23] studied the performance of a vane with shower head film cooling. Turbulence had different effects on the film cooling characteristics on the pressure and suction sides. In modern aero engines, turbine vanes with full coverage film cooling are used. Cheng et al. [24] studied the effects of mainstream turbulence on the film cooling effectiveness of cylindrical holes. In an early study, Metzger et al. [25] studied the film cooling characteristics on a plane surface with full coverage film cooling holes. Gao et al. [26] investigated the film cooling performance of a blade with axial-shaped holes. Fu et al. [27] studied the full coverage film cooling performance on a turbine vane at different mass flow rate ratios and mainstream Reynolds number conditions.

There is still a lack of understanding of film cooling characteristics on the entire vane surfaces under different turbulence intensities. Meanwhile, the effects of mainstream turbulence on the full coverage film cooling effectiveness of a shaped hole vane are not clear. Furthermore, the full coverage film cooling effectiveness analysis of turbine vane with chevron shaped holes has not been studied in open literatures. The primary objective of this paper is to investigate the effects of mainstream turbulence intensity on the full coverage film cooling effectiveness distribution in the different regions of two enlarged actual three-dimensional twisted vanes

with cylindrical or shaped holes. The film cooling effectiveness at three mainstream turbulence intensities (*Tu*=2%, 9% and 15%) and three mass flow ratios (*MFR* =5.5%, 8.4% and 12.5%) was measured.

2. Experimental Setup

Figure 1 gives the schematic of the wind tunnel used in the present study. The width of the inlet of the test section is 161 mm as shown in Fig. 2(a). And the height of the inlet is 90.2 mm. The inlet velocity of the mainstream was measured by a pitot tube at the pressure measuring point. In this experiment, the mainstream velocity was maintained at 20 m/s in the test section entry. The Reynolds number is 1.2×10^5 based on the mainstream inlet velocity and the vane chord length. A turbulence grid was designed to be removable in the upstream of the test section to get different turbulence intensities. The turbulence measuring points are shown in Fig. 1. The details of the turbulence grid are shown in Figure 2(b). The inlet mainstream turbulence intensities were measured to be 9% and 15% using a hot-wire anemometer by adjusting the location of the grid, and the corresponding distances from the grid to the leading edge of the vane were 312 mm and 213 mm, respectively. The turbulence intensity was measured to be 2% without the grid. There were two thermocouples in the tunnel to measure the mainstream temperature. The mass flow rate was adjusted by the mass flowmeters.

In the test section, an enlarged three-dimensional twisted vane model was centrally located in the two-passage linear cascade as shown in Fig. 2(a). Table 1 gives the parameters of the vane cascade. The test vane is made of resin material with low thermal conductivity. Static pressure measurement positions and the film hole row positions are shown in Fig. 3.

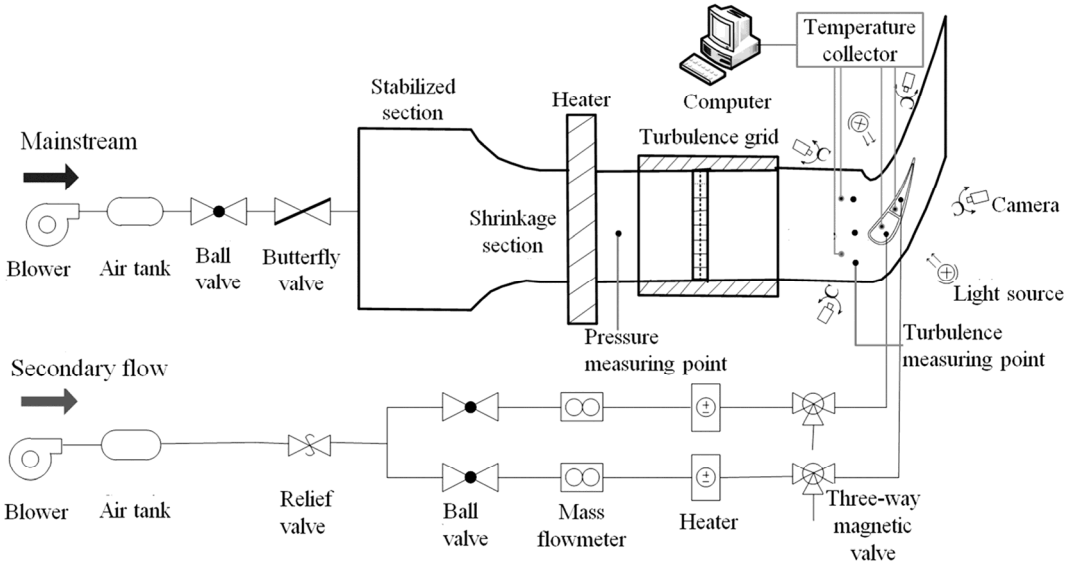

Fig. 1 The schematic diagram of the wind tunnel

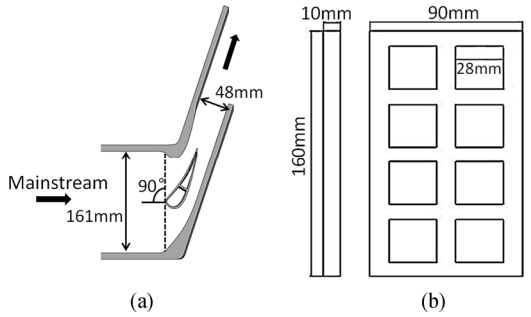

Fig. 2 Test section (a) and turbulence grid (b) schematic

Table 1 The vane geometric parameters

Chord /mm	Pitch /mm	Span /mm	Inlet angle	Exit angle	Setting angle
95.7	80.5	90.2	90°	18.5°	30°

There are 3, 8 and 7 rows of film holes on the suction side, the leading edge and the pressure side, respectively. The test vane has two cavities to feed 18 film hole rows. Fig. 4(a) and (b) show the picture of the cylindrical hole vane and the shaped hole vane, respectively. The outside surface of the vane is sprayed with black paint as background color, and then with the thermal liquid crystal which can measure the surface temperature by displaying distinctive colors at particular temperature. For the shaped hole vane, the film hole rows (4-11) are laid-back shaped holes. The film hole rows (12, 14, 15, 17, 18) on the pressure side and the film hole rows (1, 2) on the suction side are chevron shaped holes. The configurations of laid-back hole and chevron shaped hole are shown in Fig. 5. Fig. 6 shows the unfolded surface pictures of the test vanes. The *S/C* is the ratio of vane arc

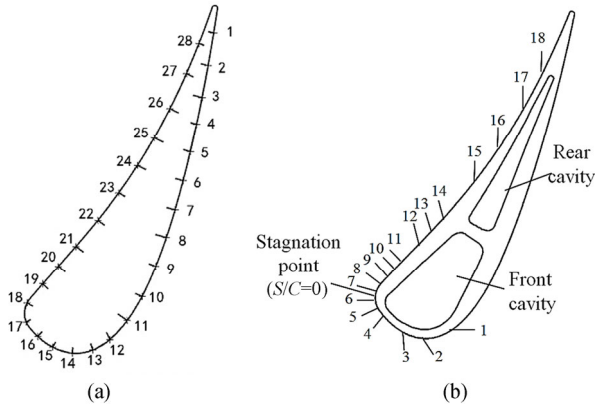

Fig. 3 Static pressure measuring positions (a) and the film hole row positions (b) in the midspan of vane

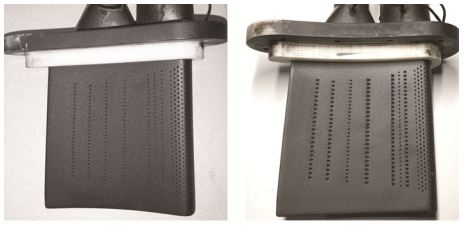

Fig. 4 Picture of cylindrical hole (a) and shaped hole (b) film cooling vanes

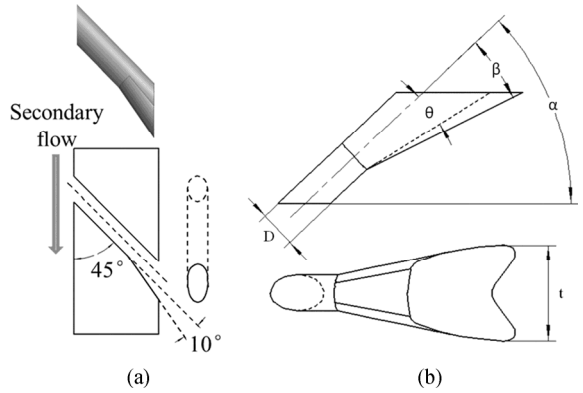

Fig. 5 Configurations of the laid-back shaped hole (a) and chevron shaped hole (b)

length to the chord length. *S/C*=0 is the position of the stagnation point. *S/C*<0 and *S/C*>0 represent the pressure side and suction side, respectively. The *H/C* is the ratio of vane height to the chord length. *H/C*=0 is the mid-span of the vane. The detailed geometry parameters of the film holes are shown in Table 2. On the suction side, the 3rd row of film holes has a compound angle of 50° in the down direction. The eight rows of holes on the leading edge have a radially inclined angle of 45° in the down direction and are all orthogonal to the local outside surface of vane in the direction of the mainstream. On the pressure side, the 13th row of holes has a compound angle of 45° in the down direction.

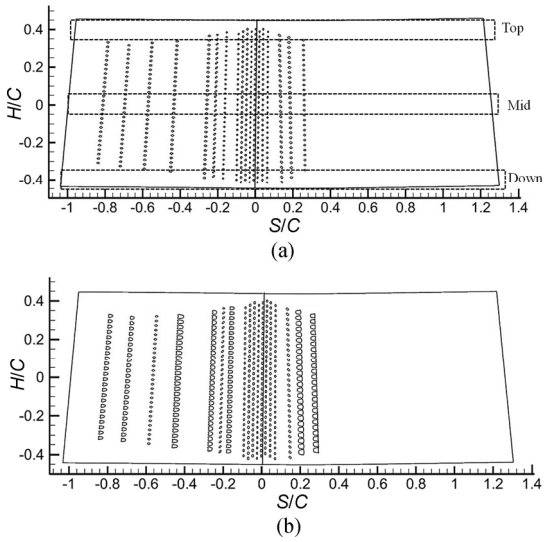

Fig. 6 Unfolded picture of the film hole positions on vane surface

Table 2 Geometry parameters of the film holes

Hole number	D/mm	α/°	β/°	θ/°	t/mm
1	0.85	40	16	10	2.25
2	1.0	50	16	10	2.25
3	0.85	60	-	-	-
4	0.7	90	10	-	-
5	0.85	90	10	-	-
6	0.85	90	10	-	-
7	0.85	90	10	-	-
8	0.7	90	10	-	-
9	0.85	90	10	-	-
10	0.85	90	10	-	-
11	0.7	90	10	-	-
12	0.7	45	18	14	1.66
13	0.7	40	-	-	-
14	0.85	40	8	4	2.2
15	0.85	40	12	10	2.04
16	0.85	40	-	-	-
17	0.85	40	12	6	1.86
18	0.85	35	12	6	1.82

As shown in Fig. 1, the cameras were located at two locations for the pressure side, one location for the leading edge and one location for the suction side. The experimental data obtained from each individual camera were analyzed with Matlab and synthesized to recover the effectiveness distribution on the curved surface. During the calibration, the calibration vane was covered

by the checkerboard pattern paper. The internal corners in the checkerboard were used as targets to calibrate the coordinate on the curved surface. Fig. 7 shows the sketch of coordinate transformation of the film cooling effectiveness results on the suction side. The three-dimensional results on the vane surface were transformed to the planar contours.

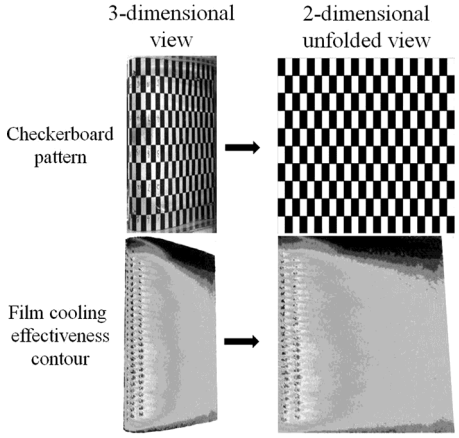

Fig. 7 The sketch of coordinate transformation of the film cooling effectiveness results (suction side)

3. Test Conditions and Data Analysis Method

3.1 Test conditions

The cascade inlet Reynolds number, secondary flow mass flow rate ratio and mainstream turbulence intensity are defined as

$$Re = \rho_g V_g C / \mu_g \tag{1}$$

$$MFR = \frac{m_{c1} + m_{c2}}{m_g} \tag{2}$$

$$Tu = v' / \overline{v} \tag{3}$$

where C is the vane chord. m_{c1} and m_{c2} are the mass flow rates of the front and rear cavity. m_g is the mass flow rate of mainstream in one cascade passage. v' and $\overline{v}$ are the fluctuation velocity and time mean velocity of the mainstream, respectively.

Experiments are performed to investigate the effect of the turbulence intensity at different mass flow rate ratios. The detailed test conditions are shown in Table 3.

Table 3 Test conditions

Re	120000
MFR	5.5%, 8.4%, 12.5%
Tu	2%, 9%, 15%

3.2 Data analysis method

3.2.1 Static pressure data

The pressure coefficient is defined as

$$C_p = \frac{P - P_\infty^*}{P_\infty^* - P_0} \tag{4}$$

The local static pressure was measured with the pressure taps located at the midspan of the vane. The difference between P_∞^* and P_0 was obtained by the pitot tube.

3.2.2 Transient liquid crystal technique

The transient thermal liquid crystal technique was used in the present study. The use of transient liquid crystal technique was firstly introduced by Vedula and Metzgar [28]. After that, Drost et al. [29] and Shih et al. [30] further developed it.

The film cooling effectiveness is defined as

$$\eta = \frac{T_g - T_{aw}}{T_g - T_c} \tag{5}$$

The details of data reduction can be seen in [31].

3.3 Measurement uncertainty

The error analysis of film cooling effectiveness was carried out using the method of Kline and McClintock [32]. In this study, the temperature errors are $\Delta T_g = \Delta T_c = \Delta T_w = \pm 0.2$°C. The uncertainty of the material property is $\Delta\sqrt{\rho c \lambda} = \pm 20$. The uncertainty of the time is Δt=0.1 s. These errors have been assessed based on the method of Liu et al. [28]. The relative uncertainty in local film cooling effectiveness was about ±15% at η=0.1 and ±3% at η=0.7. The relative uncertainty in the pressure coefficient was 4.7%. The relative uncertainties in the mainstream turbulence intensity and Reynolds number were ±3% and ±1.9%, respectively. The relative uncertainty of mass flow rate ratio was 2%.

4. Results and Discussion

4.1 Static pressure results

Fig. 8 shows the pressure coefficient distributions in the midspan of the vane at the turbulence intensities of 2%, 9% and 15%. The results show that the pressure coefficient distributions for the three turbulence intensities are nearly consistent to each other in the region of $0<S/C<0.3$, meanwhile the pressure coefficient decreases sharply in the mainstream direction. In the region of $S/C>0.3$, adverse pressure gradient occurs on the suction side along mainstream direction, which indicates that the mainstream decelerates in this region. On the pressure side, the pressure coefficient decreases along the mainstream direction. The pressure coefficient in Tu=9% and 15% is lower than that in Tu=2% condition, which reflects the larger pressure loss of the mainstream in high turbulence.

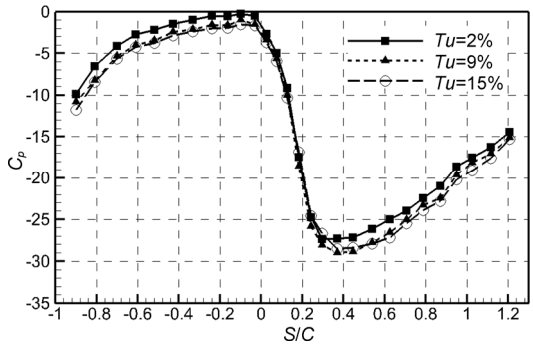

Fig. 8 Pressure coefficient distributions

4.2 Film cooling effectiveness results

The film cooling performance is different at different regions of the vane surface. To get more comprehensive results, the contour plot is divided into three regions to be discussed: top, mid and down regions. The positions of the three regions are shown in Fig. 6(a). The detailed ranges of regions are given in Table 4. The spanwise breadth of each region is about 10% of the vane height. It should be noted that the following discussions of spanwise averaged film cooling effectiveness are based on the three regions.

Table 4 Ranges of different vane regions

	Top region	Mid region	Down region
H/*C*	(0.37,0.46)	(−0.045,0.045)	(−0.46, −0.37)
S/*C*	(−0.96,1.22)	(−0.98,1.27)	(−1,1.29)

4.2.1 Low mass flow rate ratio condition (*MFR*=5.5%)

Fig. 9 shows the film cooling effectiveness on the vane in different mainstream turbulence intensity conditions. The mass flow rate ratio is 5.5% and keeps constant. The corresponding average film cooling effectiveness results in different regions are shown in Fig. 10. From the results in Fig. 9, we can see that the film cooling effectiveness distributions have some similar features in different mainstream turbulence intensity conditions. The film cooling effectiveness in the just downstream of the film holes is high, and then it decreases in the streamwise direction due to the coolant dissipation. The film cover region shrinks on the suction side for all test conditions. It is mainly due to the effect of the passage vortex in the cascade. The passage vortex on the suction side gathers the coolant to the middle region of suction surface. On the pressure side, the passage vortex makes the coolant spread to the top and down region. In the stagnation region (−0.1<*S*/*C*<0.1) on the leading edge, the film cooling effectiveness is relatively lower due to the mainstream impingement. It can be noted that the film cooling outflow trajectories near the leading edge incline downwards. As mentioned above, the 8 rows of film holes on the leading edge have radial angle, meanwhile the 13rd row of film holes on the pressure side and the 3rd row of film holes on the suction side have compound angle, which makes coolant have the velocity component in the down direction and some coolant gathers in the down region. The film cooling results at low mainstream turbulence in Fig. 9(b) show that the chevron shaped holes on the pressure and suction side increase the film cooling effectiveness and film coverage, because the vertical velocity component of film jets is decreased and the spanwise velocity component is increased by the expansion and the larger exit area of the chevron hole divergent section.

By comparing the contour plots in different turbulence intensity conditions, it can be seen that the change of turbulence intensity has an obvious effect on the film cooling effectiveness distributions. For the cylindrical hole vane, the high mainstream turbulence provides higher film cooling effectiveness on the leading edge, especially in the lower half (region A, marked in Fig. 9(a)). The reason is that the high turbulence intensity enhances the mixing of coolant and mainstream. The coolant spreads around and some of the coolant attaches to the wall surface near the stagnation region. However, for the shaped hole vane, the film cooling effectiveness on the leading edge decreases with turbulence increasing, because the coolant with lower momentum is easy to dissipate due to the enhanced mixing of coolant and mainstream at high mainstream turbulence. On the pressure and suction sides, the effects of mainstream turbulence of the film cooling effectiveness are similar. The coolant trajectories at low mainstream turbulence intensity are long and clear, while the coolant trajectories become shorter and vaguer in the high mainstream turbulence conditions. The reason is that the higher mainstream turbulence intensifies the interaction of coolant jets and mainstream and makes the vortexes larger, which accelerates the coolant dissipation. The film cooling effectiveness on the pressure side decreases obviously with the increase of the turbulence because of the more intense coolant mixing. More mainstream air intervenes in the coolant flow field due to larger movement. Likewise, in the second half of suction side (region B, marked in Fig. 9(a)), the film cooling effectiveness at *Tu*=9% and 15% is lower.

The results in Fig. 10(a, b) and Fig. 10(e, f) show that the spanwise average film cooling effectiveness in the top and down regions of the pressure side (*S*/*C*<−0.2) decreases at high mainstream turbulence due to the enhanced coolant dissipation. The results also show that the average film cooling effectiveness in the top region on the pressure side increases in the streamwise direction, while that in the down region decreases in the streamwise direction. The reason is that the coolant in the top region

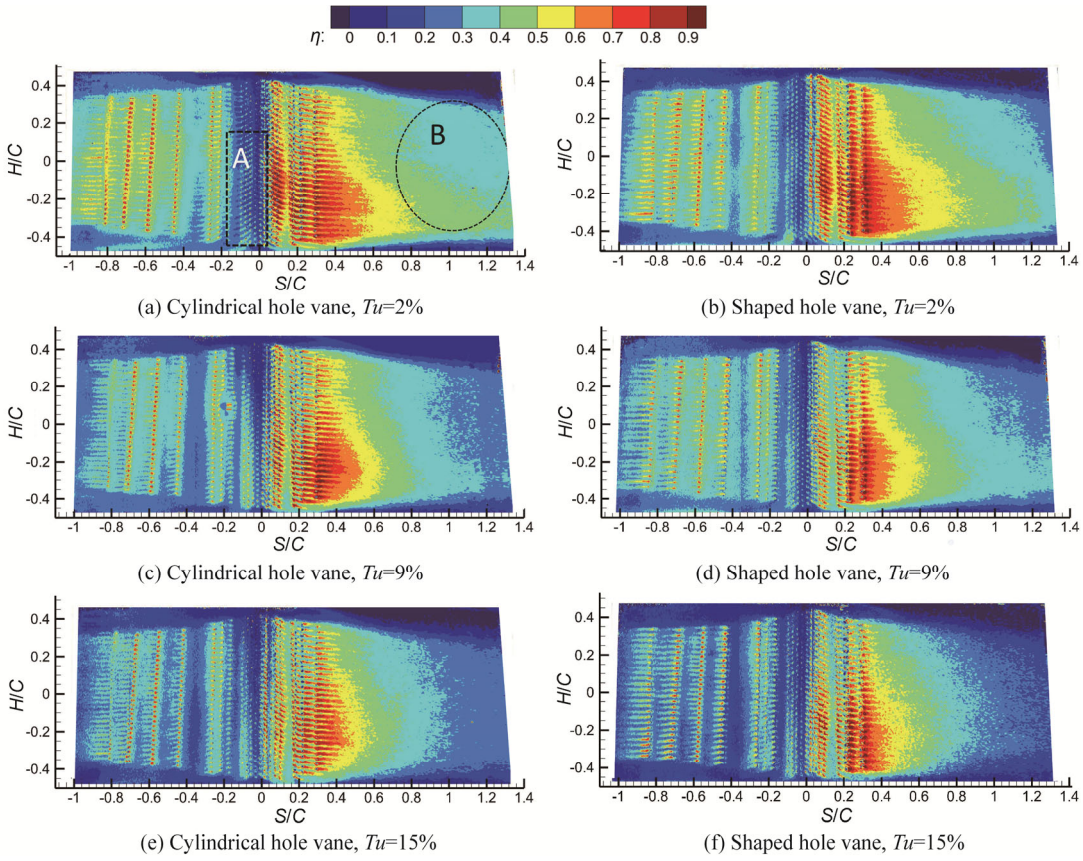

(a) Cylindrical hole vane, *Tu*=2%
(b) Shaped hole vane, *Tu*=2%
(c) Cylindrical hole vane, *Tu*=9%
(d) Shaped hole vane, *Tu*=9%
(e) Cylindrical hole vane, *Tu*=15%
(f) Shaped hole vane, *Tu*=15%

Fig. 9 Film cooling effectiveness distributions; *MFR*=5.5%

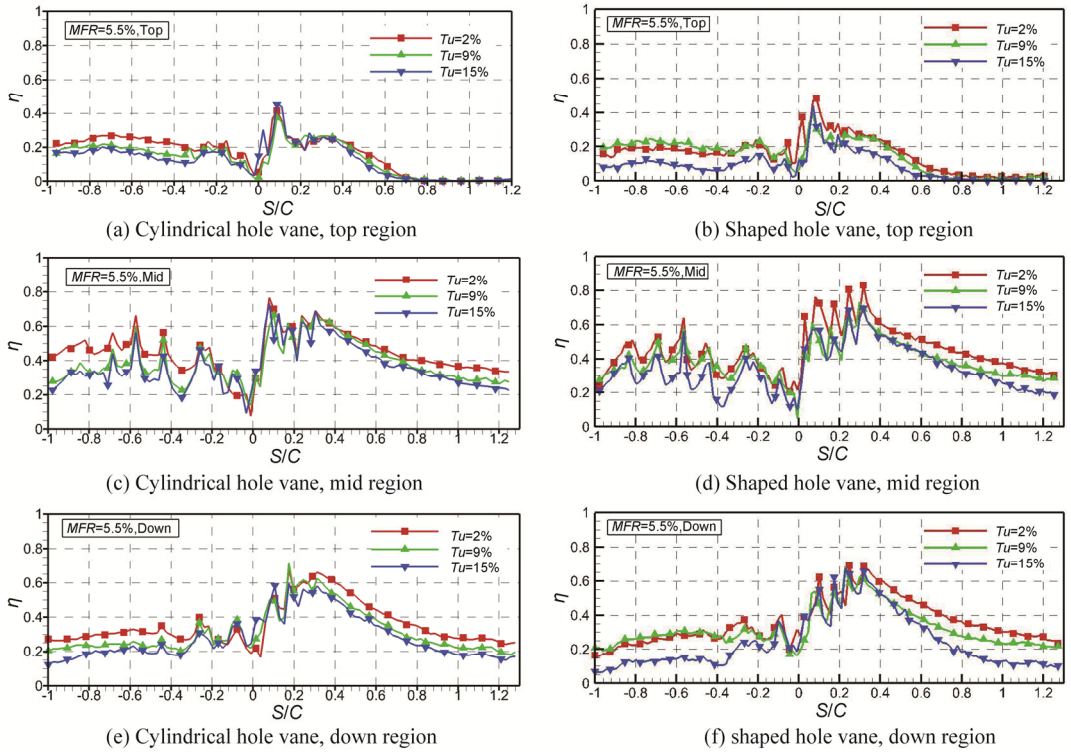

(a) Cylindrical hole vane, top region
(b) Shaped hole vane, top region
(c) Cylindrical hole vane, mid region
(d) Shaped hole vane, mid region
(e) Cylindrical hole vane, down region
(f) shaped hole vane, down region

Fig. 10 Spanwise average film cooling effectiveness in different regions; *MFR*=5.5%

mainly comes from the film cooling hole rows on the pressure side by the effect of passage vortex. The film cooling effectiveness in the top region increases in the streamwise direction with more film cooling hole rows supplying coolant to the top region. However, the coolant in the down region mainly comes from the film holes on the leading edge and the 13th row of film holes which have a compound angle.

4.2.2 Medium mass flow rate ratio condition (*MFR*= 8.4%)

Fig. 11 shows the film cooling effectiveness distributions in *MFR*=8.4% condition. The corresponding average film cooling effectiveness results in different regions are shown in Fig. 12. The results in Fig. 11 show that for the cylindrical hole vane, the film cooling effectiveness on the leading edge increases and then decreases with the mainstream turbulence intensity increasing. It is because of that the film jets from the leading edge have larger normal momentum component in *MFR*=8.4% condition and more coolant lifts off the wall surface. The increase of mainstream intensity enhances the mixing of the lift-off film jets and mainstream in the hole exit, and some of the lift-off coolant diffuses to the wall surface. However, the film cooling effectiveness on the leading edge decreases in *Tu*=15% condition due to the excessive mixing of coolant and mainstream.

In the middle region of the pressure side, similar to the *MFR*=5.5% condition, the cooling effectiveness of *Tu*=2% is higher than that of *Tu*=9% and 15% conditions. In the top region of pressure side for the cylindrical hole vane, the results in Fig. 11 and Fig. 12(a) show that the difference of film cooling effectiveness at different turbulence intensities is small. The reason is that the effects of the high mainstream turbulence have two aspects: on the one hand, the high turbulence enhances the coolant dissipation in the top region, which decreases the film cooling effectiveness; on the other hand, more coolant mixes with the mainstream and then diffuses to the top region under the effect of passage vortex at high mainstream turbulence, which increases the film cooling effectiveness. The two effects balance each other out in *MFR*=8.4% condition. For the shaped hole vane, the film cooling effectiveness in the top region of pressure side still decreases with mainstream turbulence increasing as shown in Fig. 12(b). In the down region of pressure side for both vanes, similar to the low *MFR* condition, the film cooling effectiveness at low mainstream turbulence intensity is higher as shown in Fig. 12(e, f).

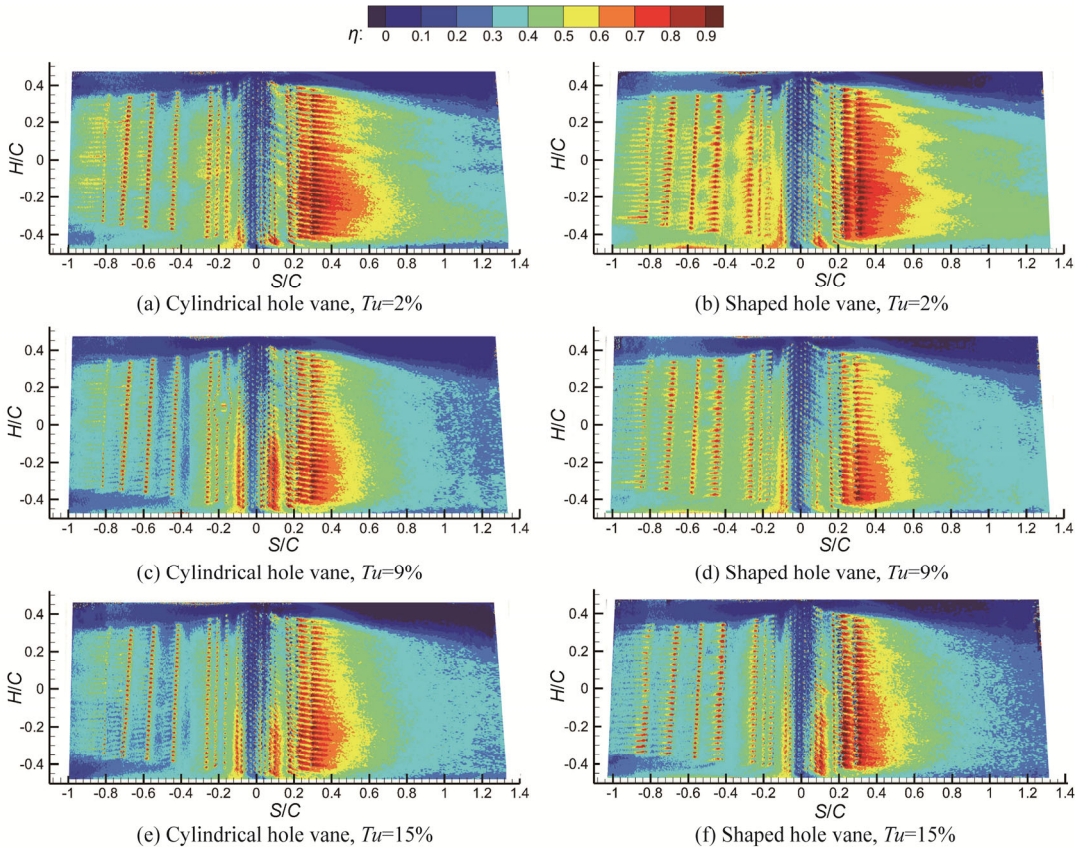

Fig. 11 Film cooling effectiveness distributions, *MFR*=8.4%

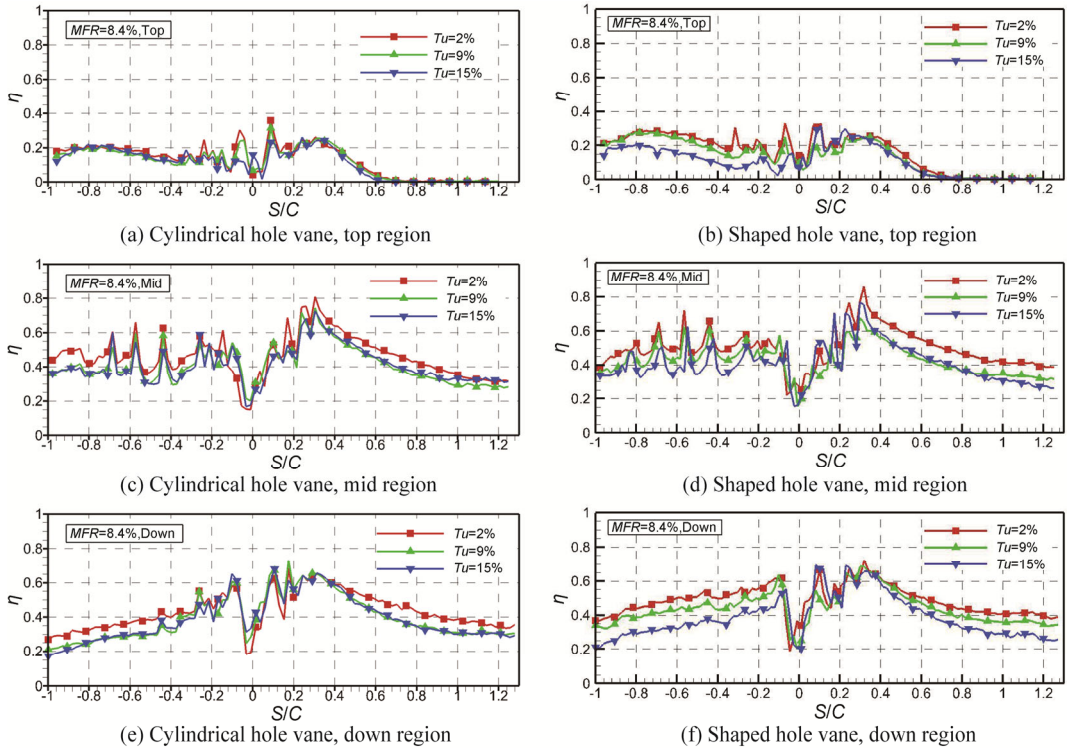

(a) Cylindrical hole vane, top region (b) Shaped hole vane, top region

(c) Cylindrical hole vane, mid region (d) Shaped hole vane, mid region

(e) Cylindrical hole vane, down region (f) Shaped hole vane, down region

Fig. 12 Spanwise average film cooling effectiveness in different regions, *MFR*=8.4%

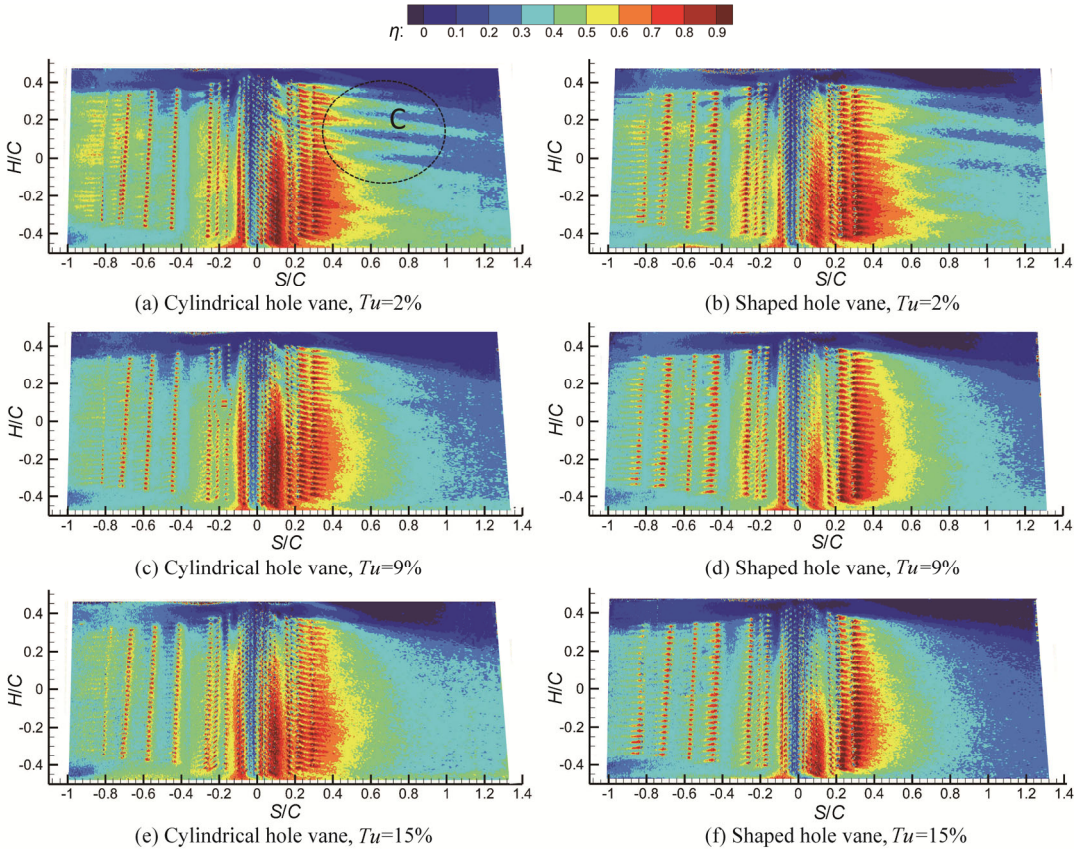

(a) Cylindrical hole vane, *Tu*=2% (b) Shaped hole vane, *Tu*=2%

(c) Cylindrical hole vane, *Tu*=9% (d) Shaped hole vane, *Tu*=9%

(e) Cylindrical hole vane, *Tu*=15% (f) Shaped hole vane, *Tu*=15%

Fig. 13 Film cooling effectiveness distributions, *MFR*=12.5%

On the second half of suction side, the highest film cooling effectiveness is obtained in *Tu*=2%, but the difference between the film cooling effectiveness at *Tu*=9% and *Tu*=15% is small. In general, for *MFR*=8.4% condition, the effect of increasing mainstream turbulence intensity becomes saturated when mainstream turbulence intensity increases from 9% to 15%.

4.2.3 High mass flow rate ratio condition (*MFR*=12.5%)

Fig. 13 shows the film cooling effectiveness distributions in *MFR*=12.5% condition. The corresponding average results in different regions are shown in Fig. 14. The results show that the increase of mainstream turbulence intensity decreases the film cooling effectiveness in the mid region of pressure side. However, the difference between the film cooling effectiveness in different turbulence conditions becomes smaller. It is because of that high mass flow rate ratio makes the adjacent film jet vortexes interact more sharply, which leads to the connection of the film cooling jets. Meanwhile, the distribution of film hole rows on the pressure side is dense. The superposition effect of film hole rows enhances the domination of the coolant on the pressure side, which provides better film protection from the mainstream entrainment. In the top and down region on the pressure side of the cylindrical hole vane, the high mainstream turbulence increases the film cooling effectiveness, which is different from that at low mass flow rate ratio. The reason is that the high mainstream turbulence enhances the interaction of coolant and mainstream, so more coolant diffuses into the mainstream and then flows to the top region and down region under the effect of passage vortex.

Fig. 13(a) and (b) shows that the results on the suction side (region C, marked in Fig. 13(a)) appears to be wavy at *Tu*=2% for both vanes while there is no such distribution in the medium and high mainstream turbulence intensity conditions. Fig. 6 shows that the 3rd row of film holes has a compound angle of 50° in the down direction. The film jets from the film hole rows in the downstream are perturbed by the film jets from the 3rd film hole row. Meanwhile, the vortexes of the film jets are stronger in the larger region at high mass flow rate ratio. The film jets interfere with each other and form a distinct wavy distribution on the suction side. The high turbulence promotes the lateral spreading of coolant jets and makes the coolant coverage more uniform. Fig. 14(c) shows that the highest average film cooling effectiveness in the region of *S/C*>0.4 for the cylindrical hole vane is obtained at *Tu*=15%, which is different from that in *MFR*=5.5% and 8.4% conditions. The reason is that the high turbulence makes the film jets merge early on the suction side at high mass flow rate ratio. Thus a wider coolant thermal field establishes in the downstream region on the suction side, which weakens the coolant dissipation and slows the decrease of film cooling effectiveness in the streamwise direction.

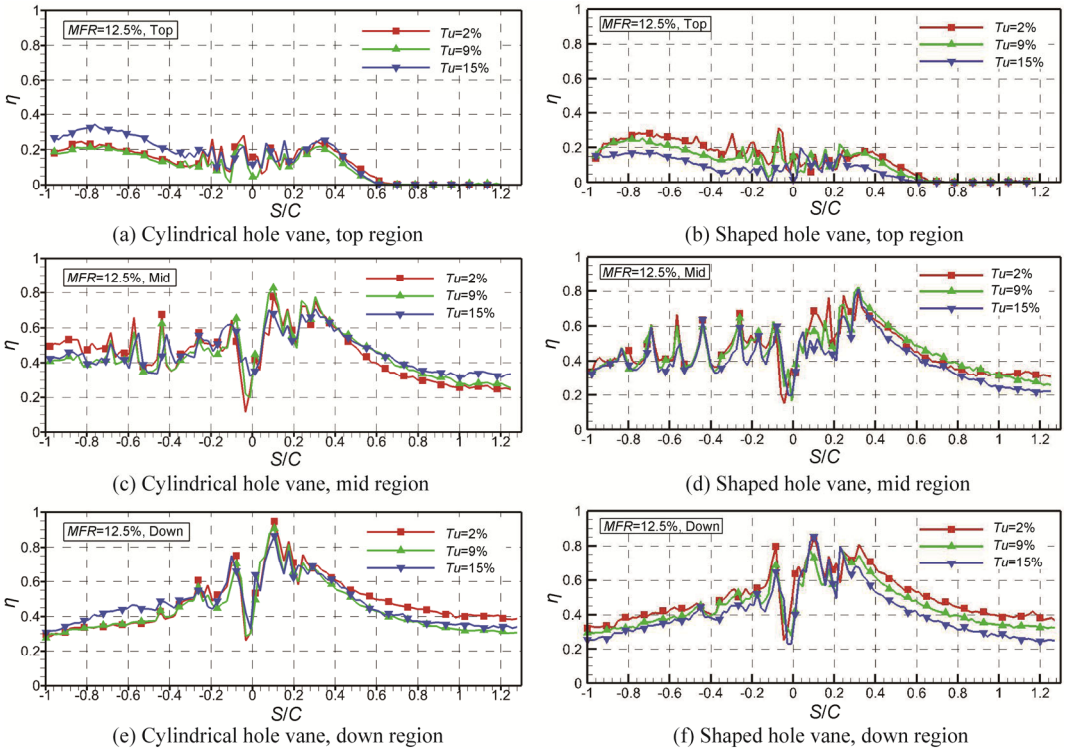

(a) Cylindrical hole vane, top region (b) Shaped hole vane, top region

(c) Cylindrical hole vane, mid region (d) Shaped hole vane, mid region

(e) Cylindrical hole vane, down region (f) Shaped hole vane, down region

Fig. 14 Spanwise average film cooling effectiveness in different regions, *MFR*=12.5%

For the shaped hole vane, Fig. 14(d) shows that the film cooling effectiveness in the middle chord region of suction side increases slightly with mainstream turbulence increasing from 2% to 9%. But in general, the film cooling on the suction side of the shaped hole vane decreases with mainstream turbulence increasing. By comparing the film cooling effectiveness results of shaped hole vane with those of the cylindrical hole vane at high mass flow rate ratio, we can see that the film cooling effectiveness of shaped vane decreases to be lower than that of cylindrical hole vane at the high mainstream turbulence of 15% except for the just downstream of film holes.

4.2.4 Area average film cooling effectiveness

Fig. 15 shows the area average film cooling effectiveness of the whole vane surface in different conditions. The results in Fig. 15(a) show that the area average film cooling effectiveness of cylindrical hole vane decreases with mainstream turbulence increasing in low and medium mass flow rate ratio conditions, while the area average film cooling effectiveness decreases first and then increases with mainstream turbulence increasing in the high mass flow rate ratio of 12.5%. The reason is that the high mainstream turbulence intensity increases the film cooling effectiveness in the top and down region of pressure side and the second half of suction side in *MFR*=12.5% condition. The results in Fig. 15(a) also show that the increase of area average film cooling effectiveness becomes saturated when mass flow rate ratio increases from 8.4% to 12.5% in *Tu*=2% condition. However, the area average film cooling effectiveness increases significantly with mass flow rate ratio increasing in *Tu*=9% and 15% conditions.

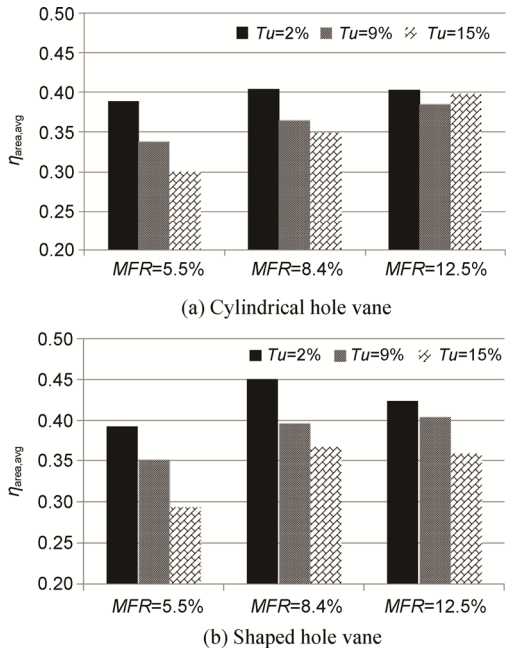

(a) Cylindrical hole vane

(b) Shaped hole vane

Fig. 15 Area average film cooling effectiveness

The results in Fig. 15(b) show that the area average film cooling effectiveness of shaped hole vane is always higher than that of cylindrical hole vane at low and medium mainstream turbulence intensities, but it is lower than that of the cylindrical hole vane obviously at the high mass flow rate ratio and high mainstream turbulence intensity condition. The reason is that the dispersive coolant from the shaped holes is more affected by high mainstream turbulence, which leads to more coolant dissipation.

5. Conclusions

The effect of mainstream turbulence intensity on the three-dimensional distribution of film cooling effectiveness for two full coverage film cooling vanes with cylindrical or shaped holes has been experimentally investigated. Three turbulence intensities (*Tu*=2%, 9% and 15%) and three mass flow rate ratios (*MFR*=5.5%, 8.4% and 12.5%) were tested. The main findings are as follows:

(1) Mainstream turbulence intensity has different effects on the film cooling effectiveness distributions in different regions of the vane surface; meanwhile, the effects are different at different secondary flow mass flow rate ratios.

(2) For the cylindrical hole vane, the film cooling effectiveness in the top region and down region of the pressure side decreases with mainstream turbulence intensity increasing in *MFR*=5.5% condition, while the effects of the increase of mainstream turbulence are exactly opposite in *MFR*=12.5% condition. In the middle region of pressure side, the film cooing effectiveness decreases with the increase of the mainstream turbulence at all mass flow rate ratios.

(3) On the leading edge of the cylindrical hole vane, the film cooling effectiveness is increased by the increase of mainstream turbulence.

(4) The film cooling effectiveness on the suction side of cylindrical hole vane decreases with mainstream turbulence increasing at *MFR*=5.5% and 8.4%. However, the high mainstream turbulence increases the film cooling effectiveness in the second half of the suction side in *MFR*=12.5% condition.

(5) For the shaped hole vane, the increase of mainstream turbulence generally decreases the film cooling effectiveness at all mass flow rate ratios.

This study reveals the influence rule of the mainstream turbulence on the film cooling effectiveness in the different regions of the three-dimensional vane surface at different mass flow rate ratios. The results would guide the designs of engineering heat transfer with application in gas turbine blade/vane cooling.

Acknowledgment

The authors acknowledge gratefully the financial support from National Basic Research Program of China (China 973 Program) under number of 2013CB035702.

References

[1] Bunker R.S., Evolution of turbine cooing, ASME Turbo Expo 2017, Charlotte, North Carolina, USA, 2017, paper No. GT2017-63205.

[2] Wieghardt K., Hot-Air discharge for de-icing, AAF Translation (2nd Ed.), Report No. F-TS-919-RE, Wright Field, Ohio, 1946.

[3] Goldstein R.J., Film cooling, Advances in Heat Transfer, 1971, 7: 321–379.

[4] Andrews G.E., Alikhanizadeh M., Tehrani B.F., Hussain C.I., and Azari M.S.K., Small diameter film cooling holes - the influence of hole size and pitch, International Journal of Turbo & Jet Engines, 1988, 5(1–4): 61–72.

[5] Guo S.M., Lai C.C., Jones T.V., Oldfield M.L.G., Lock G.D., Rawlinson A.J., The application of thin-film technology to measure turbine-vane heat transfer and effectiveness in a film-cooled, engine-simulated environment, International Journal of Heat & Fluid Flow, 1998, 19(6): 594–600.

[6] Li G.C., Wang H.F., Zhang W., Kou Z.H., Xu R.S., Film cooling performance of a row of dual-fanned holes at various injection angles, Journal of Thermal Science, 2017, 26(5): 453–458.

[7] Dittmar J., Schulz A., Wittig S., Adiabatic effectiveness and heat transfer coefficient of shaped film cooling holes on a scaled guide vane pressure side model, International Journal of Rotating Machinery, 2014, 10(5): 345–354.

[8] Thole K.A., Sinha A.K., Bogard D.G., Crawford M.E., Mean temperature measurements of jets with a crossflow for gas turbine film cooling application. International Symposium on Transport Phenomena and Dynamics of Rotating Machinery, Honolulu, USA, 1992: 69–85.

[9] Nirmalan V., Hylton L.D., An experimental study of turbine vane heat transfer with leading edge and downstream film cooling, Journal of Turbomachinery, 1990, 112: 477–487.

[10] Han J.C., Dutta S., Ekkad S.V., Gas turbine heat transfer and cooling technology, Taylor and Francis, New York, USA, 2000.

[11] Eriksen V.L., Goldstein R.J., Heat transfer and film cooling following injection through inclined circular tubes, Journal of Heat Transfer, 1974, 96(2): 239–245.

[12] Lebedev V.P., Lemanov V.V., Misyura S.Y., Terekhov V.I., Effects of flow turbulence on film cooling efficiency, International Journal of Heat & Mass Transfer, 1995, 38(11): 2117–2125.

[13] Li G., Chen Y., Kou Z., Zhang W., Zhang G., Mechanism of film cooling with one inlet and double outlet hole injection at various turbulence intensities, International Journal of Turbo & Jet Engines, 2018, 35(1): 1–9.

[14] Schroeder R.P., Thole K.A., Effect of high freestream turbulence on flowfields of shaped film cooling holes, Journal of Turbomachinery, 2016, 138(9): 091001.

[15] Goldstein R.J., Stone L.D., Row-of-holes film cooling of a convex and a concave wall at low injection angles, Journal of Turbomachinery, 1997, 119(3): 574–579.

[16] James R.W., Joshua B.A., Convex curvature effects on film cooling adiabatic effectiveness. Journal of Turbomachinery, 2013, 136: 061015

[17] Funazaki K.I., Kawabata H., Okita Y., Free-stream turbulence effects on leading edge film cooling, International Journal of Gas Turbine, Propulsion and Power System, 2012, 4(1): 43–50.

[18] Liu J.J., Bai T., et al., Leading edge film cooling enhancement for an inlet guide vane with fan-shaped holes. Journal of Thermal Science, 2010, 19(6): 514–518.

[19] Andrews G.E., Bazdiditehrani F., Small diameter film cooling hole heat transfer - The influence of the number of holes, ASME Gas Turbine and Aeroengine Congress and Expo, Toronto, Canada, 1989, paper No. 89-GT-7.

[20] Abdullah K., Funazaki K.I., Experimental investigations on aero-thermal interaction of film cooling air ejected from multiple shallow angle cooling holes: effect of freestream turbulence, ASME Turbo Expo 2013, San Antonio, Texas, USA, 2013, paper No. GT 2013-95346.

[21] Kingery J., Ames F., Full coverage shaped hole film cooling in an accelerating boundary layer with high free-stream turbulence, Journal of Turbomachinery, 2015, 138(7): 071002.

[22] Ames F.E., Aspects of vane film cooling with high turbulence: part i—heat transfer. Journal of Turbomachinery, 1998, 120(4): 768–776.

[23] Ames F.E., Aspects of vane film cooling with high turbulence: part ii—adiabatic effectiveness, Journal of Turbomachinery, 1998, 120(4): 777–784.

[24] Cheng L., Zhu H., Jiang R., et al., The effect of turbulence intensity on full coverage film cooling for a turbine guide vane, 2018 Joint Propulsion Conference, Cincinnati, Ohio, 2018, paper No. 2018-4523.

[25] Metzger D.E., Takeuchi D.I., Kuenstler P.A., Effectiveness and heat transfer with full-coverage film cooling, Journal of Engineering for Power, 1973, 95(3): 180−184.

[26] Gao Z., Narzary D., Mhetras S., Han J.C., Full-coverage film cooling for a turbine blade with axial-shaped holes, Journal of Thermophysics & Heat Transfer, 2012, 22(1): 50–61.

[27] Fu Z.Y., Zhu H.R., Liu C.L., Liu C., Li Z., An experimental investigation of full-coverage film cooling effectiveness and heat transfer coefficient of a turbine guide vane in a linear transonic cascade, ASME Turbo Expo 2016, Soule, South Korea, 2016, paper No. GT2016-56839.

[28] Vedula R.J., Metzger D.E., A method for the simultaneous determination of local effectiveness and heat transfer distributions in three temperature convection situations, ASME Gas Turbine and Aeroengine Congress and Expo 1991, Orlando, FL, USA, 1991, paper No. 91-GT-345.

[29] Drost U., Bolcs A., Hoffs A., Utilization of the transient liquid crystal technique for film cooling effectiveness and heat transfer investigations on a flat plane and a turbine airfoil. ASME Gas Turbine and Aeroengine Congress and Expo 1997, Orlando, FL, USA, 1997, paper No. 97-GT-026.

[30] Shih T.I.P., Chyu M.K., Gogineni S., Yu Y., Yen C.H., Film cooling effectiveness and heat transfer coefficient distributions around diffusion shaped holes, Journal of Heat Transfer, 2002, 124(5): 820–827.

[31] Liu C., Zhu H., Bai J., and Xu D., Film cooling performance of converging-slot holes with different exit-entry area ratios, ASME Turbo Expo 2009, Orlando, FL, USA, 2009, paper No. GT 2009-59002.

[32] Kline S.J., Describing uncertainties in single-sample experiments, Mechanical Engineering, 1953, 75(1): 3–8.